

A reactive oxygen species-generating, cyclooxygenase-2 inhibiting, cancer stem cell-potent tetranuclear copper(II) cluster

Received 00th January 20xx,
Accepted 00th January 20xx

C. Lu,^{a,b} K. Laws,^a A. Eskandari,^a and K. Suntharalingam^{a*}

DOI: 10.1039/x0xx00000x

www.rsc.org/

Tetranuclear copper(II) complexes containing multiple diclofenac and Schiff base moieties, 1-4 are shown to kill bulk cancer cells and cancer stem cells (CSCs) with low micromolar potency. The most effective complex, 1 elicits its cytotoxic effect by elevating intracellular reactive oxygen species (ROS) levels and inhibiting cyclooxygenase-2 (COX-2) expression.

Cancer stem cells (CSCs) are a distinct subpopulation of tumour cells that have high clonal long-term repopulation and self-renewal capacity.^{1,2} The quiescent, slow-cycling, and stem-like properties of CSCs enable them to survive current therapeutic regimens (which are often designed to target proliferating bulk cancer cells) and instigate tumour regrowth.³ CSCs are also linked to metastasis due to their inherent plasticity to reversibly transition between stem cell-like cells and non-stem cell-like cells.^{4,5} The clinical implication of CSCs means that cancer treatments must have the ability to remove heterogeneous cancer population in their entirety, including bulk cancer cells and CSCs, otherwise CSC-mediated relapse could occur. Although a great deal of effort has gone into identifying CSC therapeutic targets such as cell surface markers, organelles, dysregulated signalling pathways, and aspects of their microenvironment,⁶ there is still no clinically approved agent (chemical or biological) that can simultaneously remove bulk cancer cells and CSCs. Most of the CSC specific small molecules undergoing clinical trials are organic in nature,⁷ however, we and others have shown that metal complexes also display attractive anti-CSC and -bulk cancer cell properties.⁸⁻¹⁵

Our previous work has shown that reactive oxygen species (ROS) elevation in combination with cyclooxygenase-2 (COX-2) inhibition by mononuclear copper(II)-nonsteroidal anti-inflammatory drug (NSAID) complexes enables CSC and bulk cancer cell toxicity.^{9,10,13} The success of this strategy is attributed to the vulnerability of CSCs and bulk cancer cells to

changes in their intracellular redox state^{16,17} and the overexpression of COX-2^{18,19} in certain CSCs and bulk cancer cells. Here, we have sought to improve CSC and bulk cancer cell activity by developing tetranuclear copper(II) complexes bearing multiple diclofenac moieties (a COX-2 inhibitor with anti-metastatic potential)^{20,21} and Schiff base ligands (a well-known ROS mediator once coordinated to copper).^{22,23} Specifically, four copper(II) centres, four diclofenac moieties, and two Schiff base ligands were used (within a single cluster) to modulate ROS generation power and COX-2 inhibition.

The tetranuclear copper(II) complexes, **1-4** were synthesized, as outlined in Scheme S1, by refluxing the appropriate Schiff base ligand, **L¹⁻⁴** with two equivalence of Cu(NO₃)₂·3H₂O and diclofenac sodium in methanol (pH 7, adjusted by triethylamine) for 24 h. The complexes were isolated as green solids in reasonable yields (48-60%), and characterised by UV-Vis and infrared spectroscopy, and elemental analysis (see ESI). Single crystals of **1** suitable for X-ray diffraction studies were obtained by slow diffusion of diethyl ether into an acetonitrile:DMF (100:1) solution of **1** (CCDC 1548878, Fig. 1 and S1). Selected bond distances and bond angles data are presented in Table S1-2. The structure consists of four copper(II) centres, two Schiff base ligands, four diclofenac moieties, and two bridging hydroxyl groups. As

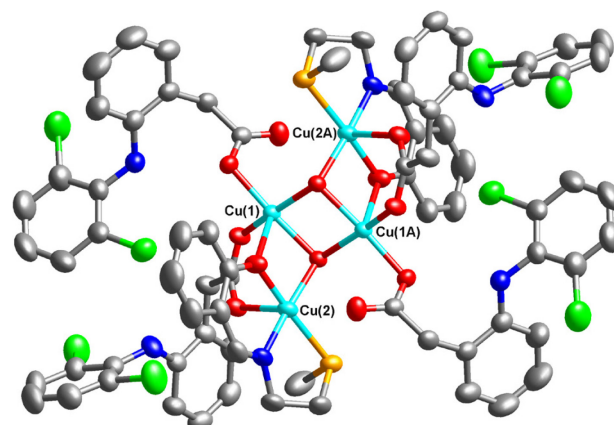


Fig. 1 X-ray structure of a tetranuclear copper(II) complex, **1** comprising of four diclofenac moieties and two Schiff base ligands. Ellipsoids are shown at 50% probability, Cl atoms are shown in green, O in red, C in grey, N in dark blue, S in yellow, and Cu in light blue. H atoms and co-crystallizing solvent molecules have been omitted for clarity.

^a Department of Chemistry, King's College London, London, SE1 1DB, United Kingdom. E-mail: kogularamanan.suntharalingam@kcl.ac.uk

^b College of Biological, Chemical Sciences and Engineering, Jiaxing University, Jiaxing 314001, China

† Footnotes relating to the title and/or authors should appear here.

Electronic Supplementary Information (ESI) available: [details of any supplementary information available should be included here]. See DOI: 10.1039/x0xx00000x

depicted in Fig. 1 and S1, Cu(1)/Cu(1A) and Cu(2)/Cu(2A) display different coordination environments. Cu(1)/Cu(1A) exhibits a five coordinate, distorted triangular bipyramid geometry whereas Cu(2)/Cu(2A) displays a five coordinate, distorted square-based pyramidal structure. The different copper(II) coordination environments is borne out in the slightly shorter distance of Cu(1)–Cu(1A) compared to Cu(1)–Cu(2). The average Cu–O (2.01 Å), Cu–S (2.39 Å), and Cu–N (1.95 Å) bond distances are consistent with bond parameter for related copper(II) complexes.^{24–26}

The stability of **1**, taken a representative member of the tetranuclear copper(II) complexes, in biologically relevant solutions was assessed using UV-Vis spectroscopy and high resolution ESI mass spectrometry. In Tris-HCl (pH 7.4)/DMSO (200:1), **1** (50 μM) is moderately stable over the course of 24 h at 37 °C (Fig. S2). In PBS (pH 7.4)/DMSO (200:1) and sodium acetate (pH 5.12)/DMSO (200:1) solutions, **1** (50 μM) is stable up to 4 hours at 37 °C, after which degradation is clearly observed (Fig. S3–4). In the presence of ascorbic acid (10 equivalents in PBS), a cellular reductant, the absorption of **1** (50 μM) changed markedly over the course of 24 h at 37 °C (Fig. S5). Specifically, the strong band at 270 nm, associated to ligand-centred π–π* transitions decreased and was replaced by a broad band at 260 nm and shoulder at 278 nm. The latter is reminiscent of free diclofenac (25 μM, Fig. S6). Lower energy bands at 320 nm and 365 nm corresponding to metal-perturbed π–π* transitions associated to **L**¹ (Fig. S6) also decreased, suggesting a possible change in the copper oxidation state and coordination environment. ESI mass spectrometry studies under the same conditions revealed peaks corresponding to [diclofenac+K]⁺ (335.0113 *m/z*) and [diclofenac-H][–] (294.0097 *m/z*) in the positive and negative mode respectively (Fig. S7 and S8). This shows that diclofenac is released under reducing conditions. Peaks with the appropriate isotopic pattern, associated to mononuclear copper complexes with various ratios of diclofenac and **L**¹ were also observed (Fig. S8 and S9), implying that **1** does not remain as a tetranuclear entity under reducing conditions. Upon incubating concentrated solutions of **1** (250 μM) with ascorbic acid (2.5 mM) in PBS/DMSO (95:5) for 24h at 37 °C, the d-d transition band (647 nm) associated to the copper(II) centre disappeared indicative of reduction to copper(I) (Fig. S10). This was further proved by the addition of bathocuproine disulfonate (BCS, 2 equivalence), a strong copper(I) chelator, which produced a characteristic absorption band at 480 nm corresponding to [Cu^I(BCS)₂]^{3–} (Fig. S11).²⁷ Collectively the UV-Vis and ESI mass spectrometry studies suggest that the copper centres in **1** are reduced from Cu(II) to Cu(I) under biologically relevant conditions and that diclofenac is liberated.

The bulk breast cancer cell (HMLER) and CSC (HMLER-shEcad) potency of **1–4** after 72 h incubation was determined using the MTT [3-(4,5-di-methylthiazol-2-yl)-2,5-diphenyltetrazolium bromide] assay. IC₅₀ values (concentrations required to reduce cell viability by 50%) were determined from dose–response curves (Fig. S12–15) and are summarized in Table 1. All of the tetranuclear complexes, **1–4** displayed equal toxicity towards CSC-enriched HMLER-shEcad

cells and bulk cancer-enriched HMLER cells, in the low micromolar range. The advantage of **1–4** over CSC-selective compounds such as salinomycin (Table 1),²⁸ is that they have the potential to remove whole cancer cell populations (bulk cancer cells and CSCs) with a single dose. CSC-selective compounds need to be administered in combination with bulk cancer-selective agents (at the appropriate dose) to elicit a similar response. Control cytotoxicity studies showed that the potency of diclofenac, CuCl₂, and **1** pre-incubated with 10 equivalents of ascorbic acid for 24 h (**1** + AA, reduced/degradation products) towards HMLER and HMLER-

Table 1. IC₅₀ values of **1–4**, diclofenac, CuCl₂, **1** preincubated with 10 equivalents of ascorbic acid for 24 h, and salinomycin against HMLER and HMLER-shEcad cells determined after 72 h incubation (mean of three independent experiments ± SD). ^a Taken from reference 9.

Compound	HMLER IC ₅₀ / μM	HMLER-shEcad IC ₅₀ / μM
1	8.4 ± 0.2	8.6 ± 0.3
2	13.1 ± 0.3	14.4 ± 0.2
3	13.0 ± 0.7	13.1 ± 0.3
4	8.3 ± 0.5	8.4 ± 0.1
diclofenac	> 100	37.1 ± 2.0
CuCl ₂	> 100	> 100
1 + AA	> 100	83.0 ± 8.9
salinomycin ^a	11.4 ± 0.4	4.2 ± 0.4

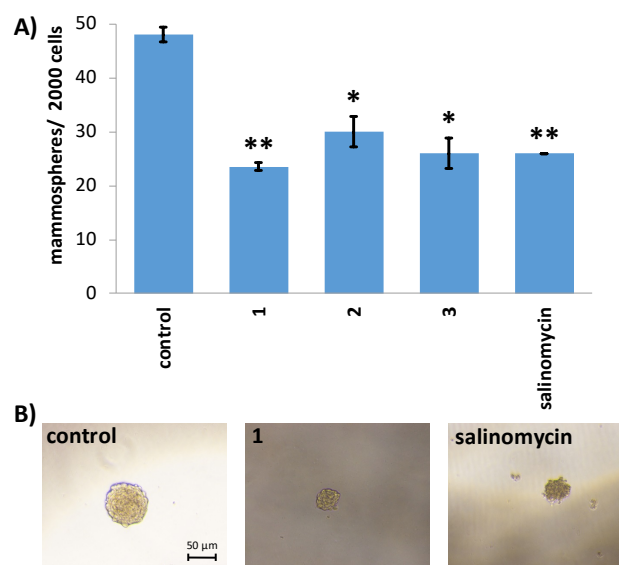


Fig. 2 (A) Quantification of mammosphere formation with HMLER-shEcad cells untreated and treated with **1–3** and salinomycin at their respective IC₂₀ values for 5 days. Error bars = SD and Student *t*-test, * = *p* < 0.05, ** = *p* < 0.01. (B) Representative bright-field images (× 10) of the mammospheres in the absence and presence of **1** and salinomycin at their respective IC₂₀ values.

shEcad cells was significantly lower than **1** (Table 1 and Fig. S16–18). This suggests that the cytotoxicity of **1** is likely to result from intact **1** rather than its individual components

(diclofenac and copper) or the reduced/degradation products (**1** + AA).

The mammosphere assay was performed to determine the ability of **1-3** to inhibit the formation of spheroids comprising of breast CSCs. This method serves as a reliable readout for CSC potency and in vivo potential, given that three-dimensional systems are more representative of solid tumours compared to monolayer cell cultures.²⁹ The addition of **1-3** (at the IC₂₀ value) to single cell suspensions of HMLER-shEcad cells significantly ($p < 0.05$) reduced the number and size of mammospheres formed after 5 days incubation (Fig. 2 and S19). Notably, **1** displayed the highest inhibitory effect, reducing the number of mammospheres formed by 51% compared to the untreated control. This is comparable to the effect of salinomycin (46% reduction in mammosphere formed), an established mammosphere-potent agent (Fig. 2). Upon treatment of single cell suspensions of HMLER-shEcad cells with diclofenac and CuCl₂ (at the IC₂₀ value for 5 days), the number and size of mammospheres formed was largely unaffected (Fig. S20-21). The colorimetric resazurin-based reagent, TOX8 was used to measure the ability of **1-3** to reduce mammosphere viability. The IC₅₀ values (concentration required to decrease mammosphere viability by 50%) of **1-3** were in the micromolar range (Fig. S22 and Table S3). Notably, **1** exhibited the greatest mammosphere-potency (IC₅₀ = 27.9 ± 1.3 μM) within the series, comparable to salinomycin (IC₅₀ = 18.5 ± 1.5 μM). Diclofenac and CuCl₂ were relatively non-toxic towards mammospheres (IC₅₀ > 133 μM, Fig. S23, Table S3). This suggests that mammosphere potency of **1** is likely to result from intact **1** rather than its individual components (diclofenac and copper). Overall the cytotoxicity and mammosphere studies show that **1-3**, in particular **1**, can effectively inhibit CSC growth in monolayer and three-dimensional cell culture systems.

Cell uptake studies were conducted to identify bulk breast cancer cell and CSC permeability. HMLER and HMLER-shEcad cells were treated with **1-4** (10 μM for 24 h) and the copper content was determined by inductively coupled plasma mass spectrometry (ICP-MS). As depicted in Fig. 3 and S24, **1-4** are readily taken up by HMLER and HMLER-shEcad cells (> 48 ppb of Cu/ million cells). Strikingly, **1** displayed up to 6-fold higher

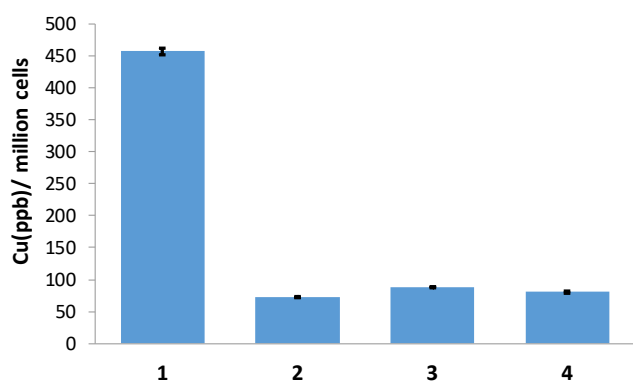


Fig. 3 Copper content in HMLER-shEcad cells treated with **1-4** (10 μM for 24 h). The copper content was determined by ICP-MS.

uptake by HMLER-shEcad cells and 2-fold higher uptake by

HMLER cells than **2-4**, suggesting that the addition of the methoxy group on the Schiff base ligand hinders bulk cancer cell and CSC uptake. No direct correlation could be drawn between cellular uptake and bulk cancer or CSC cell cytotoxicity. Control cellular uptake studies showed that CuCl₂ and **1** + AA (reduced/degradation products) were taken up to a lesser extent than **1** by HMLER-shEcad cells under identical conditions (10 μM for 24 h) (Fig. S25). Diclofenac was also shown to not traffic large quantities of copper into HMLER-shEcad cells (Fig. S25). This suggests that **1** is taken up better by CSCs as the intact cluster rather than as the reduced/degraded products (**1** + AA). For **1**, the complex with the greatest uptake, fractionation studies were carried out with HMLER-shEcad cells (treated with 10 μM for 24 h), to determine cell localisation (Fig. S26). A significant amount of internalised **1** was detected in the cytoplasm (35%). A relatively lower, but nevertheless appreciable amount of **1** was found in the nucleus (11%). The data also revealed that a large portion of **1** (48%) became trapped in the cell membrane. This is could be due to the large size and high intrinsic lipophilicity of **1**. Overall, the fractionation studies suggest that **1**-induced toxicity is more likely to result from deleterious action within the cytoplasm rather than the nucleus.

The tetranuclear complexes were expected to increase intracellular ROS levels and thereby induce cell death. To determine the ability of **1** to produce ROS in HMLER-shEcad cells, 6-carboxy-2',7'-dichlorodihydrofluorescein diacetate (DCFH-DA), a well-established ROS indicator was used. HMLER-shEcad cells treated with **1** (20 μM) displayed a noticeable

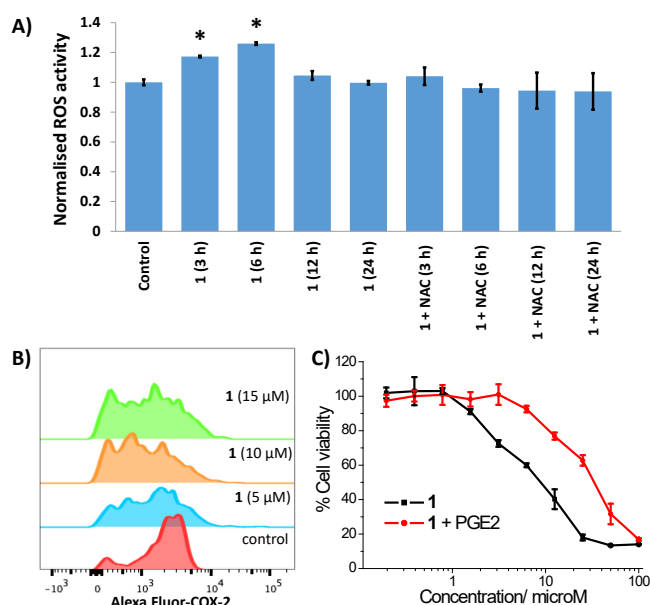


Fig. 4 (A) Normalised ROS activity in untreated HMLER-shEcad cells (control) and HMLER-shEcad cells treated with **1** (20 μM for 3, 6, 12, and 24 h) and co-treated with **1** (20 μM for 3, 6, 12, and 24 h) and *N*-acetylcysteine (2.5 mM for 3, 6, 12, and 24 h). Error bars represent standard deviations and Student *t* test, * = $p < 0.05$. (B) Representative histograms displaying the green fluorescence emitted by anti-COX-2 Alexa Fluor 488 nm antibody-stained HMLER-shEcad cells treated with LPS (2.5 μM) for 24 h (red) followed by 48 h in media containing **1** (5 - 15 μM, blue, orange, and green). (C) Representative dose-response curves for the treatment of HMLER-shEcad cells with **1** after 72 incubation in the presence and absence of PGE2 (20 μM).

increase in ROS levels after 3 h (17%) and 6 h (26%) exposure (Fig. 4A). Prolonged exposure of **1** (20 μ M for 12 or 24 h) did not significantly increase ROS levels compared to untreated control cells (Fig. 4A). Therefore **1**-induced ROS generation is time-dependent. Similar results have been reported for other metal complexes.³⁰ HMLER-shEcad cells treated with H₂O₂ (150 μ M for 3, 6, 12, or 24 h) exhibited a marked increase in ROS levels (7-8-fold) relative to untreated control cells (Fig. S27). Notably, both **1**- (after 6 and 3 h exposure) and H₂O₂- (after 3, 6, 12, and 24 h exposure) induced ROS production was reduced in the presence of *N*-acetylcysteine (2.5 mM), a ROS scavenger (Fig. 4A and S27). Cytotoxicity studies in the presence of *N*-acetylcysteine (2.5 mM, 72 h) showed that the potency of **1** towards HMLER-shEcad cells decreased significantly (IC₅₀ value increased from 8.6 \pm 0.3 μ M to 11.9 \pm 0.3 μ M, p < 0.05) (Fig. S28). Taken together, this suggests that **1**-induced cell death is related to intracellular ROS generation.

COX-2 is overexpressed in certain cancer cells and linked to proliferative cancer growth and resistance against traditional chemotherapy and radiotherapy.^{31,32} There is compelling evidence for a role for COX-2 in CSC biology and as a mediator of tumour repopulation and metastasis.^{18,32} Given these findings, COX-2 is now recognised as a molecular target for CSC-directed therapy. As the tetranuclear complex, **1** contains four diclofenac moieties which can potentially be released under biologically reducing conditions, flow cytometric studies were performed to determine if the mechanism of action of **1** involved COX-2 downregulation. Upon treatment of HMLER-shEcad cells pre-treated with lipopolysaccharide (LPS) (2.5 μ M for 24 h), to increase basal COX-2 levels, with **1** (5-15 μ M for 48 h), a marked decrease in COX-2 expression compared to untreated cells was observed (Fig. 4B). A decrease in COX-2 expression was also observed in HMLER-shEcad cells treated with diclofenac (20 μ M for 48 h) (Fig. S29). Overall, the flow cytometric data suggests that the cytotoxic mechanism of action of **1** may involve COX-2 downregulation. To prove this, cytotoxicity studies were carried out with HMLER-shEcad in the presence and absence of prostaglandin E2 (PGE2) (20 μ M, 72 h), the functional product of COX-2-catalysed arachidonic acid metabolism. The IC₅₀ value of **1** against HMLER-shEcad cells decreased by 3.8-fold in the presence of PGE2 (Fig. 4C), implying that **1** induces COX-2-dependent CSC death.

In summary, we report the first tetranuclear copper(II) complexes, **1-4** to simultaneously kill bulk cancer and CSCs. As **1-4** are equipotent towards bulk cancer cells and CSCs, they have the potential to remove heterogeneous tumour populations with a single dose. The representative complex, **1** is readily taken up by CSCs and induces cell death by generating intracellular ROS and downregulating COX-2 expression. Our results pave the way for the development of other multinuclear metal complexes (bearing various biologically active moieties) that can evoke bulk cancer and CSC death through distinct cellular pathways.

K.S. is supported by a Leverhulme Early Career Fellowship (ECF-2014-178). K.L. and A.E. are supported by a King's College London GTS-PhD Studentship and Faculty Graduate School International Studentship, respectively. C.L. thanks the Natural

Science Foundation of China (Grant No.21401078) for financial support. We are grateful to Prof. Robert Weinberg (Whitehead Institute, MIT) for providing the cell lines used in this study.

Notes and references

1. V. Plaks, N. Kong and Z. Werb, *Cell Stem Cell*, 2015, **16**, 225-238.
2. L. V. Nguyen, R. Vanner, P. Dirks and C. J. Eaves, *Nat. Rev. Cancer*, 2012, **12**, 133-143.
3. M. Dean, T. Fojo and S. Bates, *Nat. Rev. Cancer*, 2005, **5**, 275-284.
4. J. Marx, *Science*, 2007, **317**, 1029-1031.
5. D. R. Pattabiraman and R. A. Weinberg, *Nat. Rev. Drug Discov.*, 2014, **13**, 497-512.
6. X. Ning, J. Shu, Y. Du, Q. Ben and Z. Li, *Cancer Biol. Ther.*, 2013, **14**, 295-303.
7. J. Kaiser, *Science*, 2015, **347**, 226-229.
8. N. Aztopal, D. Karakas, B. Cevatemre, F. Ari, C. Icel, M. G. Daidone and E. Ulukaya, *Bioorg. Med. Chem.*, 2017, **25**, 269-276.
9. J. N. Boodram, I. J. McGregor, P. M. Bruno, P. B. Cressey, M. T. Hemann and K. Suntharalingam, *Angew. Chem. Int. Ed.*, 2016, **55**, 2845-2850.
10. A. Eskandari, J. N. Boodram, P. B. Cressey, C. Lu, P. M. Bruno, M. T. Hemann and K. Suntharalingam, *Dalton Trans.*, 2016, **45**, 17867-17873.
11. M. Flamme, P. B. Cressey, C. Lu, P. M. Bruno, A. Eskandari, M. T. Hemann, G. Hogarth and K. Suntharalingam, *Chemistry*, 2017, DOI: 10.1002/chem.201701837.
12. M. Gonzalez-Bartulos, C. Aceves-Luquero, J. Qualai, O. Cusso, M. A. Martinez, S. Fernandez de Mattos, J. A. Menendez, P. Villalonga, M. Costas, X. Ribas and A. Massagué, *PLoS ONE*, 2015, **10**, e0137800.
13. C. Lu, A. Eskandari, P. Cressey and K. Suntharalingam, *Chemistry*, 2017, DOI: 10.1002/chem.201701939.
14. C. T. Lum, A. S. Wong, M. C. Lin, C. M. Che and R. W. Sun, *Chem. Commun.*, 2013, **49**, 4364-4366.
15. K. Suntharalingam, W. Lin, T. C. Johnstone, P. M. Bruno, Y. R. Zheng, M. T. Hemann and S. J. Lippard, *J. Am. Chem. Soc.*, 2014, **136**, 14413-14416.
16. M. Diehn, R. W. Cho, N. A. Lobo, T. Kalisky, M. J. Dorie, A. N. Kulp, D. Qian, J. S. Lam, L. E. Ailles, M. Wong, B. Joshua, M. J. Kaplan, I. Wapnir, F. M. Dirbas, G. Somlo, C. Garberoglio, B. Paz, J. Shen, S. K. Lau, S. R. Quake, J. M. Brown, I. L. Weissman and M. F. Clarke, *Nature*, 2009, **458**, 780-783.
17. X. Shi, Y. Zhang, J. Zheng and J. Pan, *Antioxid. Redox Signal.*, 2012, **16**, 1215-1228.
18. B. Singh, J. A. Berry, A. Shoher, V. Ramakrishnan and A. Lucci, *Int. J. Oncol.*, 2005, **26**, 1393-1399.
19. B. Singh, K. R. Cook, L. Vincent, C. S. Hall, C. Martin and A. Lucci, *J. Surg. Res.*, 2011, **168**, e39-49.
20. J. A. Mitchell, P. Akarasereenont, C. Thiemeermann, R. J. Flower and J. R. Vane, *Proc. Natl. Acad. Sci. U.S.A.*, 1993, **90**, 11693-11697.
21. P. Pantziarka, V. Sukhatme, G. Bouche, L. Meheus and V. P. Sukhatme, *Ecancermedicalscience*, 2016, **10**, 610.
22. C. Marzano, M. Pellei, F. Tisato and C. Santini, *Anticancer Agents Med. Chem.*, 2009, **9**, 185-211.

23. C. Santini, M. Pellei, V. Gandin, M. Porchia, F. Tisato and C. Marzano, *Chem. Rev.*, 2014, **114**, 815-862.
24. S. Caglar, E. Dilek, B. Caglar, E. Adiguzel, E. Temel, O. Buyukgungor and A. Tabak, *J. Coord. Chem.*, 2016, **69**, 3321-3335.
25. S. Dhar, M. Nethaji and A. R. Chakravarty, *Inorg. Chim. Acta.*, 2005, **358**, 2437-2444.
26. S. Dhar, M. Nethaji and A. R. Chakravarty, *Inorg. Chem.*, 2006, **45**, 11043-11050.
27. A. A. Kumbhar, A. T. Franks, R. J. Butcher and K. J. Franz, *Chem. Commun.*, 2013, **49**, 2460-2462.
28. P. B. Gupta, T. T. Onder, G. Jiang, K. Tao, C. Kuperwasser, R. A. Weinberg and E. S. Lander, *Cell*, 2009, **138**.
29. G. Dontu, W. M. Abdallah, J. M. Foley, K. W. Jackson, M. F. Clarke, M. J. Kawamura and M. S. Wicha, *Genes Dev.*, 2003, **17**, 1253-1270.
30. M. J. Chow, C. Licon, G. Pastorin, G. Mellitzer, W. H. Ang and C. Gaiddon, *Chem. Sci.*, 2016, **7**, 4117-4124.
31. C. Sobolewski, C. Cerella, M. Dicato, L. Ghibelli and M. Diederich, *Int. J. Biochem. Cell Biol.*, 2010, **2010**.
32. L. Y. Pang, E. A. Hurst and D. J. Argyle, *Stem Cells Int.*, 2016, **2016**, 11.